Spectroscopic and theoretical studies on some new pyrrol-2-yl-chloromethyl ketones

Alina T. Dubis,*[a] Małgorzata Domagała[b] and Sławomir J. Grabowski*[c]

Received (in Montpellier, France) 23rd September 2009, Accepted 8th December 2009
First published as an Advance Article on the web 5th February 2010
DOI: 10.1039/b9nj00507b

A novel series of pyrrole-2-yl chloromethyl ketones were synthesized and studied by FT-IR, ^{1}H, ^{13}C NMR spectroscopy and DFT calculations at the B3LYP/6-311++G(d,p) level of approximation. Two stable conformations were detected in solution: s-*cis* and s-*trans* forms where the C=O group is located on the same side or the opposite side of N–H group, respectively. The conformational stability of these molecules is governed mainly by intermolecular hydrogen bonding interactions. The strength of hydrogen bonds was evaluated on the basis of ^{1}H chemical shift and infrared red shift $\Delta\nu_{N-H}$ of the stretching vibration of N–H proton donating bonds. The quantum theory of 'atoms in molecules' as well as the natural bond orbital method were applied to characterize hydrogen bonding interactions.

Introduction

Over the past few years some new carbonyl α-substituted pyrrole compounds have been investigated. Although the parent compound is experimentally well recognized[1] and has often theoretically analyzed,[2] little is still known about its derivatives and intra- and intermolecular noncovalent interactions within this group of moieties. At least, there are not many studies on interactions of such compounds. On the other hand, general studies show that intermolecular interactions strongly influence on the arrangement of molecules in crystals, especially directional hydrogen bonds.[3] It was also found that halogen bonds may be treated as counterparts of the latter interactions.[4] Recently, we have noticed the existence of C–Cl···O halogen bonds in crystal structure of 1-methylpyrrol-2-yl trichloromethyl ketone (**2**).[5]

We have analyzed other interactions of carbonyl α-substituted pyrroles, mainly different kinds of hydrogen bonds.[6] DFT calculations indicated that for the s-*cis* conformation of pyrrole-2-carboxylic acid, where N–H and C=O bonds are located at the same side of the moiety, two centrosymmetric dimers are possible.[6d] For each of them there are two equivalent hydrogen bonds. However in the first case these are two O–H···O bonds creating $R_2^2(8)$ motifs (graph-set-assignments) according to Etter's rules;[7] in the second case there are two N–H···O hydrogen bonds which form $R_2^2(10)$ motifs. These graph-set-assignments were introduced to H-bonded motifs existing in crystal structures.[7] R designates the ring and the number of atoms creating the ring is given in parentheses. Thus for $R_2^2(8)$ there are eight ring atoms linked through covalent and hydrogen bonds, *i.e.* ···H–O–C=O···H–O–C=O···, since two hydrogen bonds exist between two carboxylic groups. The superscript and subscript designate the number of proton acceptors and proton donors, respectively. For $R_2^2(8)$ there are two equivalent proton acceptor O-centers (since the dimer is linked through two equivalent molecules) and two equivalent proton donating bonds (O–H). Etter has stated that there are also other motifs,[7] C designates the chain of atoms containing hydrogen bonding which repeats in the crystal structure, S concerns intramolecular hydrogen bonds and D corresponds to a dimer where there is a single hydrogen bond.

In the case of the s-*trans* conformer of pyrrole-2-carboxylic acid, there is only the possibility of the dimer containing two equivalent O–H···O bonds within the $R_2^2(8)$ motif. X-Ray measurement was performed on the crystal structure of pyrrole-2-carboxylic acid and it was found that s-*cis* conformers exist in crystals forming the $R_2^2(8)$ and $R_2^2(10)$ motifs mentioned above.[6e] The combined experimental thermochemical and computational study of 2-pyrrolcarboxylic acid and 1-methyl-2-pyrrolecarboxylic acid was performed very recently.[8] Another example is pyrrole-2-carboxamide analyzed by experimental spectroscopic and X-ray methods as well as by DFT calculations.[9] For the latter species, the s-*cis* conformer was detected and also the existence of centrosymmetric dimers in crystals connected through N–H···O bonds was indicated.

It is worth mentioning that for all α-substituted pyrrole compounds mentioned above different theoretical techniques may be applied to analyze various interactions. These are *ab initio* and DFT calculations which allow determination of the stable monomers' and dimers' molecular structures as well as their energies. Quantum theory of 'atoms in molecules' (QTAIM) is a useful tool to analyze those interactions since the characteristics of bond critical points (BCPs) often indicate the nature of the interactions considered.[10] It was found that there are mainly strong hydrogen bonds for α-substituted pyrrole compounds, especially if $R_2^2(8)$ motifs containing O–H···O hydrogen bonds are taken into account. This was found for centrosymmetric dimers of pyrrole-2-carboxylic

[a] *Institute of Chemistry, University of Białystok, Al. J. Piłsudskiego 11/4, 15-443 Białystok, Poland. E-mail: alina@uwb.edu.pl*
[b] *Department of Chemistry, University of Łódź, ul. Pomorska 149/153, 90-236 Łódź, Poland*
[c] *Ikerbasque Research Professor, Kimika Fakultatea, Euskal Herriko Unibertsitatea and Donostia International Physics Center (DIPC), P.K. 1072, 20080 Donostia, Euskadi, Spain. E-mail: S.grabowski@ikerbasque.org*

acid, formic and acetic acid.[11] If strong hydrogen bonds are considered thus, there is the important contribution of the delocalization energy term within the binding energy and such a term is comparable with the electrostatic energy.[12] In such a case any interaction possesses characteristics of a covalent bond. For medium strength hydrogen bonds, the electrostatic energy is the most important attractive interaction energy term and that was found for N–H···O hydrogen bonds within $R_2^2(10)$ motifs of pyrrole-2-carboxylic acid.[11] The characteristics of BCPs allow determination of whether any interaction is covalent or electrostatic in nature.[13]

Furthermore, it is worth noticing that the conformation of molecules is connected to the presence of the hydrogen bond interaction as, for example, it was observed in many biological systems.[14,15] One can see that there are different conformations as well as various kinds of interactions, especially hydrogen bonds, for carbonyl α-substituted pyrroles. Hence, as a continuation of our previous study on the conformational structure of the pyrrole derivatives[6,16] and hydrogen bond interactions for these species, some new chlorine pyrrole derivatives were designed and synthesized (Scheme 1). We decided to approach the effect of alpha-bulky substituents that are big enough to inhibit rotation around C–C single bond.

In this paper we reported the synthesis of new pyrrole-2-substituted ketones (**1–6**) and their spectroscopic and structural properties. The purpose of these investigations was to establish conformational preferences of some new derivatives of 2-substituted pyrroles using spectroscopic and theoretical methods. Additionally the goal of this study was to analyze the hydrogen bonds for the species considered and particularly to determine some of their geometrical, energetic and QTAIM characteristics. The following theoretical methods were applied here: DFT method,[17] the above-mentioned QTAIM[10] and the natural bond orbitals (NBO) method.[18] To the best of our knowledge neither structural nor vibrational studies on **1–6** compounds have been carried out till now.

Experimental section

General methods

The FT-IR spectra were recorded using a Nicolet Magna IR 550 Series II Spectrometer equipped with KBr beam splitter and DTGS detector. Samples were measured in cyclohexane, CCl_4, $CHCl_3$ and acetonitrile solutions and as KBr pellets. A spectral resolution of 2 cm^{-1} was used. All solvents were dried and freshly distilled prior to use. ^1H and ^{13}C NMR spectra were recorded using a Bruker Avance II 400 MHz NMR spectrometer using $CDCl_3$ solution with TMS as an internal standard.

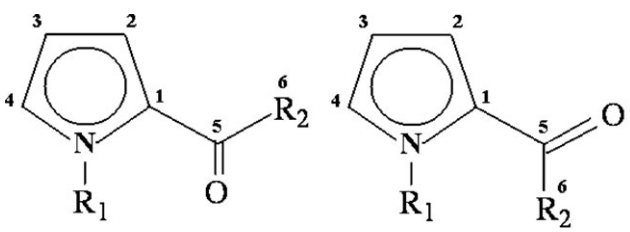

(**1**) R_1=H, R_2=CCl_3 (**2**) R_1=CH_3, R_2=CCl_3
(**3**) R_1=H, R_2=$CHCl_2$ (**4**) R_1=CH_3, R_2=$CHCl_2$
(**5**) R_1=H, R_2=CH_2Cl (**6**) R_1=CH_3, R_2=CH_2Cl

Scheme 1 Structure of the 2-substituted pyrroles. Atom numbering corresponding to that one used further in Tables is included, number 6 is the C-atom of the R_2 group. Higher conformation: s-*cis*, lower conformation: s-*trans*.

Synthesis of the pyrrol-2-yl chloromethyl ketones (1, 3, 5) and their N-methyl derivatives (2, 4, 6)

The conventional Friedel–Crafts acylation method was applied for preparation of the aromatic ketones **1–6**.[19] The title pyrroloketones were generally obtained by using acid chlorides as acylating agents and stoichiometric amounts of $AlCl_3$ as a reaction promoter. It is worth noticing that synthesis of ketones **1** and **2** were successfully carried out without any strong Lewis acid catalytic agent.

0.02 mol of trichloroacetyl chloride or dichloroacetyl chloride or chloroacetyl chloride was dissolved in 10 ml of anhydrous ethyl ether. The 0.02 mol of freshly distilled pyrrole was added dropwise and the reaction mixture was stirred for one hour at room temperature. After that time a water solution of 0.02 mol of potassium carbonate was added. The resulting mixtures were extracted twice with ether and the crude products were purified by crystallization from hexane.

Pyrrol-2-yl trichloromethyl ketone (1). IR ($CHCl_3$) ν/cm^{-1}: 3446, 3142, 3118, 3066, 1664, 1538, 1427, 1393, 1315, 1123, 1106, 1058, 1037, 882, 846. ^1H NMR ($CDCl_3$) δ (ppm): 6.41 (dd, 1H, Ar–H); 7.22 (t, 1H, Ar–H); 7.43 (dd, 1H, Ar–H); 9.57 (s, 1H, NH). ^{13}C NMR ($CDCl_3$) δ (ppm): 94.9 (CH); 111.8 (CH); 121.3 (CH); 127.5 (C), 122.8 (C); 173.2 (C). Mp = 73–75 °C.

1-Methylpyrrol-2-yl trichloromethyl ketone (2). IR ($CHCl_3$) ν/cm^{-1}: 3145, 3116, 3131, 2954, 1671, 1524, 1481, 1460, 1439, 1424, 1403, 1390, 1366, 1331, 1244, 1403, 1390, 1366, 1331, 1244, 1228, 1099, 1071, 1044, 984, 884, 848. ^1H NMR ($CDCl_3$) δ (ppm): 3.98 (s, 3H, $H_3C–N_{Ar}$); 6.21 (dd, 1H, Ar–H); 6.98 (m, 1H, Ar–H); 7.52 (dd, 1H, Ar–H). ^{13}C NMR ($CDCl_3$) δ (ppm): 38.4 (CH); 96.2 (CH); 108.8 (CH); 123.9 (CH); 133.6 (C); 121.6 (C); 172.7 (C). Mp = 65 °C.

Pyrrol-2-yl dichloromethyl ketone (3). IR ($CHCl_3$) ν/cm^{-1}: 3446, 1663, 1543, 1401, 1097, 571. ^1H NMR ($CDCl_3$) δ (ppm): 6.39 (dd, 1H, Ar–H); 6.54 (s, 1H, $CHCl_2$); 7.24 (m, 1H, Ar–H); 7.26 (dd, 1H, Ar–H); 9.84 (s, 1H, NH). ^{13}C NMR ($CDCl_3$) δ (ppm): 67.1 (CH); 111.8 (CH); 119.4 (CH); 128.4 (C), 125.9 (C); 176.9 (C). Mp = 89.2–89.8 °C.

1-Methylpyrrol-2-yl dichloromethyl ketone (4). IR ($CHCl_3$) ν/cm^{-1}: 3025, 3013, 2955, 1671, 1526, 1484, 1463, 1406, 1386, 1331, 1256, 1248, 1229, 1194, 1097, 1070, 968, 827, 800. ^1H NMR ($CDCl_3$) δ (ppm): 3.98 (s, 3H, $H_3C–N_{Ar}$); 6.23 (dd, 1H, Ar–H); 6.59 (s, 1H, $CHCl_2$); 6.99 (m, 1H, Ar–H); 7.14 (dd, 1H, Ar–H). ^{13}C NMR ($CDCl_3$) δ (ppm): 37.8 (CH); 67.9 (CH); 109.2 (CH); 121.1 (CH); 133.8 (C), 125.6 (C); 176.5 (C). Mp = 65.8–66.6 °C.

Pyrrol-2-yl chloromethyl ketone (5). IR ($CHCl_3$) ν/cm^{-1}: 3448, 3021, 1652, 1546, 1428, 1403, 1332, 1260, 1225, 1122,

1097, 1051, 930. ^{1}H NMR ($CDCl_3$) δ (ppm): 4.51 (s, 1H, CH_2Cl); 6.32 (dd, 1H, Ar–H); 7.01 (t, 1H, Ar–H); 7.15 (dd, 1H, Ar–H); 9.93 (s, 1H, NH). ^{13}C NMR ($CDCl_3$) δ (ppm): 44.3 (CH); 111.2 (CH); 117.5 (CH); 126.3 (C), 129.2 (C); 181.5 (C). Mp = 120.5 °C.

1-Methylpyrrol-2-yl chloromethyl ketone (6). IR ($CHCl_3$) ν/cm^{-1}: 3021, 2951, 1656, 1527, 1483, 1463, 1407, 1387, 1331, 1278, 1240, 1095, 1067, 972, 918. ^{1}H NMR ($CDCl_3$) δ (ppm): 3.96 (s, 3H, H_3C–N_{Ar}); 4.5 (s, 1H, CH_2Cl); 6.18 (dd, 1H, Ar–H); 6.91 (m, 1H, Ar–H); 7.01 (dd, 1H, Ar–H). ^{13}C NMR ($CDCl_3$) δ (ppm): 37.6 (CH); 45.6 (CH); 108.6 (CH); 119.8 (CH); 132.2 (C), 128 (C); 181.3 (C). Mp = 46.5 °C.

Computational details

The calculations have been performed with the Gaussian 98[20] and Gaussian 03[21] sets of codes. The B3LYP hybrid density functional was applied which combines Becke's three-parameter non-local exchange potential with the non-local correlation functional of Lee, Yang and Parr.[22] The 6-311++G(d,p) Pople-style basis set[23] was used. Thus the calculations were performed at B3LYP/6-311++G(d,p) level of approximation, including the vibrational frequencies. The Gauss-view program[24] was used to assign the calculated harmonic frequencies. The results of optimizations correspond to energy minima since no imaginary frequencies were found.

The binding energies for the analyzed dimers have been computed as the difference between the total energy of the complex and the energies of the isolated monomers and were corrected for the basis set superposition error (BSSE) using the counterpoise procedure.[25] Since the optimizations were carried out also for isolated monomers the binding energy thus includes the structural deformation energy as an effect of complexation. The binding energy is often referred to the H-bond energy, however this is a correct approach if the strongest and only meaningful molecule–molecule connection is through hydrogen bonding. All systems analyzed are linked through double N–H···O equivalent hydrogen bonds since two linked molecules are related through an inversion centre. Hence the H-bond energy is calculated here as a half of the binding energy.

The quantum theory of 'atoms in molecules'[10] is applied to determine critical points (CPs), especially bond critical points (BCPs) corresponding to H···O intermolecular interactions. The AIM2000 program[26] was used to find CPs and to determine their characteristics. The natural bond orbitals (NBO) method[18] is also applied to determine atomic charges as well as to get insight into the molecule–molecule interactions, especially the energy corresponding to the n → σ* (n(O) → σ*(N–H)) electron charge transfer. The latter energy is assumed to be mainly responsible for the existence of hydrogen bonding.[27]

Results and discussion

FT-IR spectra of the pyrrol-2-yl chloromethyl ketones (1, 3, 5) and 1-methylpyrrol-2-yl chloromethyl ketones (2, 4, 6)

The theoretical and spectroscopic studies on conformations of some 2-substituted pyrrole derivatives have shown that s-*cis* conformers, where the carbonyl group is located on the same side as N–H or N–CH_3 group, are more stable than s-*trans* forms.[6,8,9] It has been also observed that this location of the carbonyl and N–H group favors the formation of centro-symmetric dimers with two equivalent intermolecular hydrogen bonds. Scheme 1 presents the molecular structures of the ketones (**1–6**) considered in this study. All these molecules contain an O atom of the carbonyl group as an acceptor centre. There is also a hydrogen atom of a –NH group in **1**, **3** and **5** which, being electropositive, may be expected to be the Lewis acid center in hydrogen bonds. It is also known that O atoms of carbonyl groups are often involved in H-bond interactions in numerous organic crystal structures.[28] Hydrogen bonds and conformations of the new 2-substituted pyrroles mentioned above are analyzed in this study by FT-IR and NMR spectroscopy supported by theoretical calculations.

Carbonyl group stretching vibrations. Fig. 1 shows the FT-IR spectra of **1**, **3**, **5** compounds in the high frequency region of 4000–1600 cm^{-1}. In the carbonyl stretching region two intense absorption bands are observed: the $\nu_{C=O}$ of hydrogen-bonded ketone groups and the $\nu_{C=O}$ of free carbonyl groups of the s-*trans* conformers. The absorption maxima were observed at 1657, 1679 cm^{-1} for **1**, 1656, 1683 cm^{-1} for **3** and 1662, 1683 cm^{-1} for **5**. Our theoretical calculations predicted that the $\nu_{C=O}$ band of the s-*trans* form lies at a higher frequency than the $\nu_{C=O}$ band of the s-*cis*-form. Selected calculated and experimental IR data have been collected in Table 1. Having considered these calculations and our previous results,[6a] we have anticipated that the $\nu_{C=O}$ bands of the s-*cis* conformers might lie at a lower frequency and overlap with the $\nu_{C=O}$ bands of the hydrogen-bonded carbonyl group. To make our point stronger the Fourier self-deconvolution (FSD) technique[29,30] has been applied. The FSD technique has been used in order to estimate the number of bands that overlap and could not be resolved by collecting spectral data even at a higher resolution.

Fig. 2 shows two absorption bands at 1683 and 1656 cm^{-1} in the carbonyl region of IR spectra of the compound **3**. The band of lower frequency revealed an irregular shape and it probably consists of some overlapping $\nu_{C=O}$ bands. The FSD method was used in order to resolve the overlapping bands.

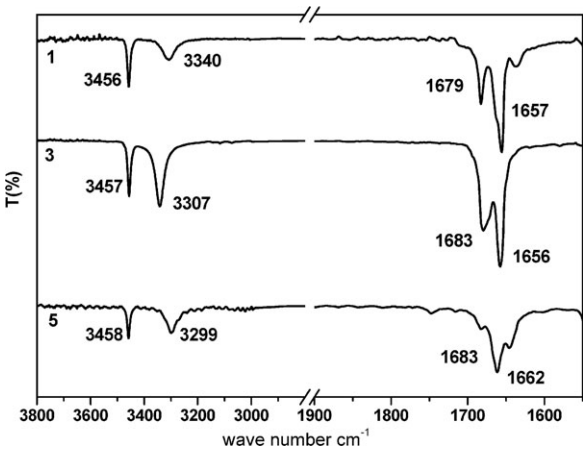

Fig. 1 Experimental IR spectra of **1**, **3** and **5** compounds run as a cyclohexane solution (0.01 M).

The high frequency absorption band at 1683 cm^{-1} was ascribed to the s-*trans* form according to theoretically predicted frequencies (Table 1). The lower frequency band observed at 1658 cm^{-1} was ascribed to the s-*cis* form and the band at 1656 cm^{-1} is due to the stretching vibration of the ketone carbonyl group that is involved in the intermolecular hydrogen bonding interaction. The absorption bands of the hydrogen-bonded C═O group at 1657 and 1662 cm^{-1} for **1** and **5** analogous compounds, respectively revealed a regular shape (Fig. 1). This is why a deconvolution procedure has been abandoned for spectra of compound **1** and **5** run in cyclohexane solution.

The dilution of the cyclohexane mother solution allows us to follow the intermolecular interaction. For **3** the $\nu_{C=O}$ band of the hydrogen-bonded C═O group observed at 1656 cm^{-1} (Fig. 3, line b) disappeared and only two bands were left: at 1683 and 1658 cm^{-1} (Fig. 3, line a). The results of the FSD procedure and dilution experiment confirm the presence of two stable conformers of **3** in the solution.

Additionally, the spectra of **1**, **3** and **5** run as cyclohexane solutions were compared with the spectra of *N*-methylated pyrroles **2**, **4** and **6**. For these two (N–CH_3 and N–H) pyrrole groups the meaningful similarities between the location of the $\nu_{C=O}$ bands were noticed. As shown in Table 1, the $\nu_{C=O}$ band of the s-*cis* forms of **3** and **4** falls at the same wave number value of 1658 cm^{-1}. Moreover, $\nu_{C=O}$ of the s-*trans* forms of **3** and **4** were also observed at the same wave number value of 1683 cm^{-1}. The similarity of the spectral pictures observed for $\nu_{C=O}$(s-*cis*) and the corresponding similarity of $\nu_{C=O}$(s-*trans*) feature in the spectra of **3** and **4** indicates that the higher-frequency band originates in the stretching vibration of the $\nu_{C=O}$(*trans*) and lower-frequency band originates in the stretching vibration of the $\nu_{C=O}$(*cis*). Having considered the observations it can be concluded that the bands at 1683 and 1658 cm^{-1} originate from $\nu_{C=O}$ of the s-*trans* and s-*cis* conformers of **3**, respectively. It is also worth noticing that, according to the theoretical prediction (Table 1), the $\nu_{C=O}$ bands of the s-*trans* and s-*cis* conformers of **3** are separated by *ca.* 18 cm^{-1}, whereas the experimentally observed separation is 25 cm^{-1}. Apart from $\nu_{C=O}$(*trans*) and $\nu_{C=O}$(*cis*) of free molecules, the absorption band of the intermolecular hydrogen-bonded carbonyl group at 1656 cm^{-1} is present in

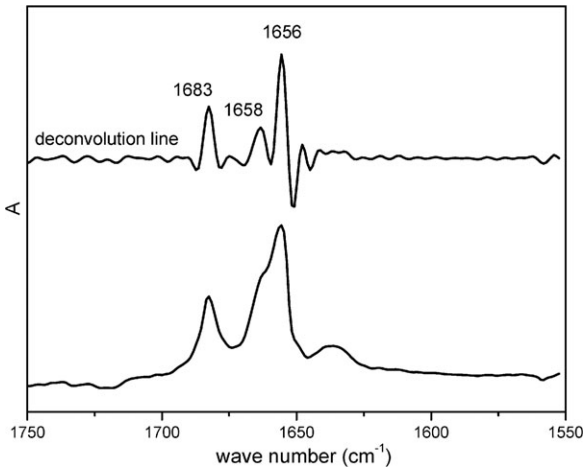

Fig. 2 The carbonyl stretching region of the FT-IR spectrum of **3** run in 0.01 M cyclohexane solution and its Fourier self-deconvolution curve.

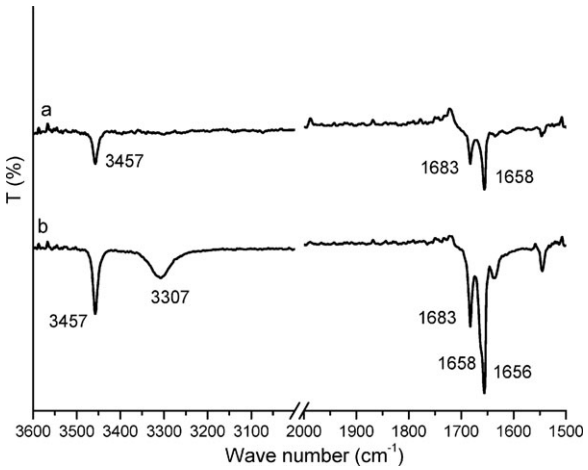

Fig. 3 Experimental FT–IR spectra of **3** run as cyclohexane solutions: (a) 0.001 M; (b) 0.01 M.

Table 1 Theoretical and experimental IR data for **1–6** pyrrol-2-yl chloromethyl ketones

	ν_{N-H}/cm^{-1}		$\nu_{C=O}$/cm^{-1}		ν^{dimer}_{N-H}/cm^{-1}		$\nu^{dimer}_{C=O}$/cm^{-1}	
Compound	Calculated B3LYP/ 6-311++G**	Exp.	Calculated B3LYP/ 6-311++G**	Exp.	Calculated B3LYP/ 6-311++G**	Exp.	Calculated B3LYP/ 6-311++G**	Exp.
1 s-*cis*	3563 (100)[e]	3456[a]	1687 (314)[e]	1670[d]	3411	3340[b], 3322[c]	1662	1657[b], 1655[c]
1 s-*trans*	3583 (95)[e]	3456[a]	1708 (281)[e]	1679[a], 1681[d]				
2 s-*cis*			1690 (236)[e]					1664[c]
2 s-*trans*			1692 (300)[e]	1681[a]				
3 s-*cis*	3561 (100)[e]	3457[a]	1692 (318)[e]	1658[a]	3357	3307[b], 3294[c]	1664	1656[b], 1653[c]
3 s-*trans*	3562 (99)[e]	3457[a]	1710 (268)[e]	1683[a]				
4 s-*cis*			1692 (302)[e]	1658[a]				1668[c]
4 s-*trans*			1690 (236)[e]	1683[a]				
5 s-*cis*	3562 (102)[e]	3458[a]	1695 (263)[e]	1662[a]	3362	3299[b], 3241[c]	1661	1646[b], 1645[c]
5 s-*trans*	3594 (67)[e]	3458[a]	1714 (235)[e]	1683[a]				
6 s-*cis*			1694 (253)[e]	1662[a]				1677[c]
6 s-*trans*			1693 (207)[e]	1683[a]				

[a] Measured as cyclohexane 0.001 M solution. [b] Measured as cycklohexane 0.01 M solution. [c] Measured as a KBr pellet. [d] Measured as CCl_4 0.001 M solution. [e] Values in parentheses are calculated intensities *A* in km mol^{-1}.

a position close to $\nu_{C=O}$ of free s-*cis* form. Moreover, the crystallographic data concerning the crystal structure of some α-substituted pyrroles[5,6,9,31] confirmed the presence of the energetically more stable s-*cis* conformers' dimers in the solid state. On the basis of these studies, the intermolecular heteronuclear N–H···O interactions were detected. Moreover it was also observed by means of dipole moment measurements that α-substituted pyrroles form intermolecular bonded centrosymmetric dimers even in a diluted solution.[6] Following these findings it was possible to assign the lowest frequency band at 1656 cm^{-1} of $\nu_{C=O}$ stretching vibration to intermolecular H-bonded molecules.

For **1** the IR spectra were run as cyclohexane and carbon tetrachloride solutions. The spectrum of the diluted 0.001 M cyclohexane solution revealed only one $\nu_{C=O}$ absorption band of a free carbonyl group at 1679 cm^{-1}, while the spectrum of a 0.001 M carbon tetrachloride solution of **1** compound showed two separated bands of free carbonyl group at 1681 and 1670 cm^{-1}. In this manner the presence of two stable forms in the solution of compound **1** has been confirmed.

Our studies have been extended to cover *N*-methyl derivatives of parent α-substituted compounds. The spectra of *N*-methylated pyrroles **2**, **4** and **6** were also analyzed and compared with the spectra of **1**, **3** and **5**. Fig. 4 shows the presence of two remarkable carbonyl bands at 1683 and 1658 cm^{-1} for **4** and two $\nu_{C=O}$ bands at 1683 and 1662 cm^{-1} for **6**, whereas for **2** only one carbonyl band at 1681 cm^{-1} appears. It means that two forms of C=O for **4** and **6** coexist in the cyclohexane solution. These results are surprising because, according to earlier investigations,[32] we expected to find only one s-*cis* conformation of *N*-methylated derivatives. Infrared spectra of compounds **2**, **4**, and **6** (Fig. 5) were also recorded in acetonitrile. Acetonitrile has been chosen because it belongs to the group of polar solvents whose acceptor number (AN) is twenty times greater than the AN of cyclohexane.[33,34] The frequencies of the $\nu_{C=O}$ band of **4** and **6** are lower in acetonitrile than in cyclohexane. The frequency shifts are 13 and 8 cm^{-1}, for the s-*trans* and the s-*cis* form of compound **6**, respectively. Furthermore, the ratio $A^{s\text{-}cis}_{C=O}/A^{s\text{-}trans}_{C=O}$ of the integrated intensities of the carbonyl bands of **6** was sensitive to solvent polarity. This ratio decreased in acetonitrile solution in comparison with less polar cyclohexane. It has been recognized[35,36] that solvent effects could be applied successfully to investigation of the equilibrium constant between rotational isomers of a molecule. Polar solvents stabilize the more polar form causing its higher proportion. Such behavior has been explained on the basis of theoretical investigation.[37] A great influence of the solvent on the thermodynamic properties of a molecule, such as enthalpy, free energy and total energy, has been found. Our previous investigations on conformations of methyl pyrrole-2-carboxylate[6c] also revealed that the population of the more polar s-*trans* form increases with the polarity of the solvent. The values of the calculated dipole moments of the conformers analyzed here are listed in Table 2. The s-*trans* forms adopt greater values than the s-*cis* forms. This means that such conformers are more polar than s-*cis* ones. Furthermore, calculated energy differences between these two conformations (Table 2) show that s-*cis* forms are more stable.

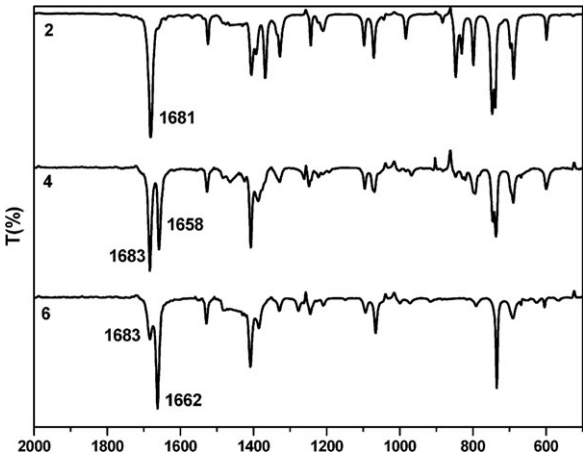

Fig. 4 Experimental FT–IR spectra of compounds **2**, **4** and **6** run as a cyclohexane solutions (0.01 M).

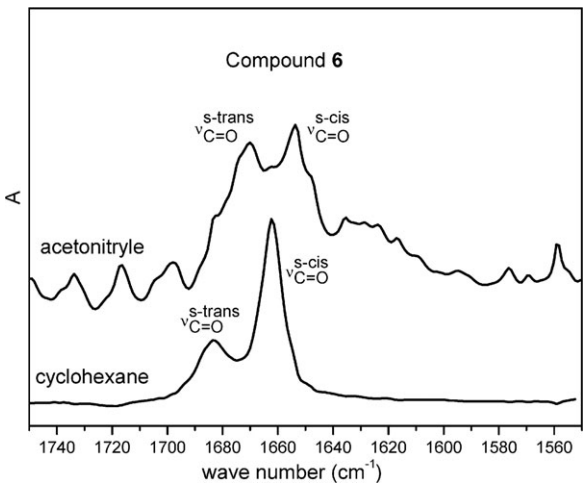

Fig. 5 Experimental FT–IR spectra in the range 1750–1550 cm^{-1} of **6** compound run as acetonitrile and cyclohexane solutions.

N–H stretching vibration. The absorption bands of the stretching vibration of the N–H group in the 3500–3200 cm^{-1} region are also very good diagnostic bands for detection of free and hydrogen-bonded molecules. The N–H bond acts as a proton donor in hydrogen-bonded complexes. In the spectra of 0.01 M cyclohexane solutions of **1**, **3** and **5**, two separated bands are observed for hydrogen-bonded and free N–H groups, respectively (Fig. 1). In a non-polar solvent like cyclohexane, the hydrogen bonds are partly broken and the spectra show additional free N–H absorption bands. For the hydrogen-bonded complexes the ν_{N-H} frequencies are downshifted if related to the corresponding values of free molecules. The frequency shifts equal 116, 150 and 159 cm^{-1} for **1**, **3** and **5** compounds, respectively. The observed shifts to lower frequencies are due to intermolecular hydrogen bonding which results in slight elongation and weakening of the N–H proton donating bond. Dilution experiments demonstrated that the nature of N–H···O interactions depends on the concentration of the solution. Considering these results, one may expect that intermolecular hydrogen bonds are present in the solutions of **1**, **3** and **5**. Earlier studies have revealed that if

Table 2 Values of dipole moments (calculated at the B3LYP/6-311++G** level of theory), energies and ΔE for the s-*cis* and s-*trans* conformers of compounds **1–6**

Compound	μ/D	E/hartree	ΔE^a/kcal mol^{-1}
1 s-*cis*	3.7929	−1741.7689165	2.55
1 s-*trans*	4.0949	−1741.7648491	
2 s-*cis*	4.1988	−1781.0835548	8.08
2 s-*trans*	4.5149	−1781.0706759	
3 s-*cis*	4.6110	−1282.1618611	4.19
3 s-*trans*	4.8286	−1282.1551927	
4 s-*cis*	4.7743	−1321.4776171	6.64
4 s-*trans*	5.7907	−1321.4670328	
5 s-*cis*	4.3186	−822.5475538	5.15
5 s-*trans*	5.6817	−822.5393359	
6 s-*cis*	4.4005	−861.8629353	6.61
6 s-*trans*	6.2019	−861.8524038	

[a] ΔE is the difference between the energies of the flat and bend conformers.

complexation leads to hydrogen bond formation the shift of the ν_{N-H} stretching vibration mode within the proton-donating molecule correlates with the strength of the H-bond.[38,39] For example, this red shift appears to be linearly correlated with the H-bond energy. The red shift of the $\Delta\nu_{N-H}$ values for **1**, **3** and **5** increases with decreasing number of chlorine atoms within the molecule. On the basis of these spectroscopic results it can be assumed that the weakest H-bonding interaction occurs for **1** while small differences between red shift values for **3** and **5** indicate that the latter ones are similar in strength.

It is also well known that hydrogen bonding may affect other physical properties such as melting points and proton ^{1}H chemical shifts of involved atoms.[27a,40] The increasing strength of hydrogen bonds in the series **1**, **3**, **5** may be responsible for the increasing melting points of these compounds which are 75, 89, 120 °C, respectively. These findings are supported by NMR spectroscopy. The NMR properties of the proton attached to highly electronegative atoms such as nitrogen are strongly influenced by the hydrogen bond interaction. It can be seen (Table 3) that the N–H proton chemical shifts are 9.57, 9.84 and 9.93 ppm for **1**, **3** and **5**, respectively. Such downfield shifts can by explain by a deshielding effect caused by the modification of the local magnetic environment at the N–H hydrogen nucleus. The latter is the effect of the increasing polarity of substituent groups –CCl_3, –$CHCl_2$ and –CH_2Cl. In comparison, dipole moments of moieties which are structurally related to the R substituent, such as $CHCl_3$, CH_2Cl_2, CH_3Cl were also calculated (Table 3). These dipole moment values increase in the following order 1.3, 2.03, 2.32 D for chloroform, methylene chloride and methyl chloride, respectively. Furthermore, for **1**, **3**, and **5** the calculated dipole moments are 4.09, 4.82 and 5.68, respectively. These observations enable us to expect that compound **5** exhibits the strongest hydrogen bond while compound **1** the weakest one. These experiments revealed that for the homogenous set of **1**, **3** and **5**, the intermolecular hydrogen bonding strength can be distinguished using the ν_{N-H} red shift values. Besides, the ν_{N-H} bands would give some additional information of rotamers which might be present. In order to check whether s-*cis* or s-*trans* rotamers could be observed in a solution, the N–H region of the spectra was analyzed using deconvolution technique (FSD). The latter analytical method was chosen since no satisfactory separation of the free N–H bands was obtained from the IR spectra taken in nonpolar solvents. The previous study on the conformation of methyl pyrrole carboxylate[6] has shown that the FSD method is useful for such a purpose. For other alpha-keto pyrroles, the separated s-*cis* and s-*trans* bands were not revealed in this spectral region. Also, the present study of the N–H stretching region has provided no confirmation of the presence of s-*trans* rotamers. We think that the reason of the absence of s-*trans* species lies in the medium that surrounds the pyrrole molecules. On the other hand, there is also a possibility that low intensity s-*trans* ν_{N-H} bands overlap with more intense s-*cis* ν_{N-H} bands. According to the theoretical predictions (Table 1), the intensity of s-*cis* ν_{N-H} bands are higher than the intensity of s-*trans* ν_{N-H} bands. On the basis of these results we can state that the N–H stretching region, in contrast to the $\nu_{C=O}$ one, does not bring valuable information on the presence or absence of two conformers in the solution.

Table 3 ^{1}H and ^{13}C NMR spectral data of compound **1–6** (5% $CDCl_3$ solutions)

Compound	**1** 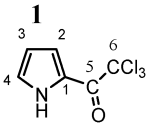	**3** 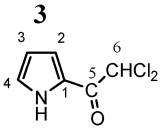	**5** 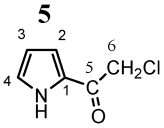	**2** 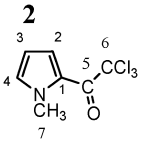	**4** 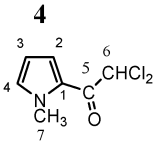	**6** 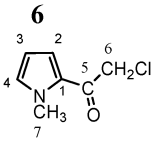
N–CH_3				3.98	3.98	3.96
N–*H*	9.57	9.84	9.93			
Ar–*H*	7.43, 7.22, 6.41	7.26, 7.24, 6.39	7.15, 7.01, 6.32	7.52, 6.98, 6.21	7.14, 6.99, 6.23	7.01, 6.91, 6.18
C*H*Cl_2		6.54			6.59	
CH_2Cl			4.51			4.5
C1	122.84	125.94	129.2	121.67	125.61	127.9
C2	121.39	119.36	117.58	123.92	121.17	119.84
C3	111.82	111.8	111.24	108.81	109.23	108.64
C4	127.5	128.35	126.3	133.58	133.85	132.25
C5	173.27	176.96	181.49	172.72	176.53	181.35
C6	94.92	67.12	44.36	96.24	67.89	45.66
C7				38.44	37.8	37.61

Vibrational properties of dimers. The solid state vibrational spectra were compared here with the spectra calculated theoretically. **1**, **3**, and **5** are expected to form dimers in concentrated solutions and in crystals, similar to earlier observations for α-substituted pyrroles.[6,9] The spectra were calculated for centrosymetric dimers linked through two symmetrically equivalent N–H···O hydrogen bonds (Fig. 6). It was observed that the N–H vibrational modes were considerably affected by the dimer formation. The calculated $\Delta\nu_{N-H}$ downshifts are equal to 152, 204 and 200 cm^{-1} for **1**, **3** and **5**, respectively, while the experimental values of the $\Delta\nu_{N-H}$ amount to 116, 150 and 159 cm^{-1} (Table 1). It follows from the experiment that $\Delta\nu_{N-H}$ grows when the number of chlorine atoms decreases. The results of calculations do not exactly reproduce this relationship. For **3** and **5** the sequence is reversed. We believe that the experimental $\Delta\nu_{N-H}$ values are influenced not only by N–H···O=C interactions but also by short Cl···O and C–H···O contacts.[3,4] It seems that the observed difference is mainly due to the complex nature of the interactions which are present in the solid state. One can also observe that there are slight differences for compounds **3** and **5**, while for compound **1** both red shifts, experimental and theoretical, are the lowest ones.

The IR spectra of the monomers and dimers are dominated also by C=O stretching bands. For dimers, red shifts of the C=O vibration are observed. The calculated values of $\Delta\nu_{C=O}$ are 25, 28 and 34 cm^{-1} for **1**, **3**, and **5** dimers, respectively, and are in good agreement with experimental spectral data (Table 1). These findings are in agreement with earlier investigations which showed that the weakening and the lengthening of C=O bonds as well as lowering of the corresponding frequency are associated with its Lewis base center properties within the hydrogen bond.[41] Additionally, a linear relationship between binding energy ΔE and $\Delta\nu_{C=O}$ has also been observed.[42] The above-mentioned findings for the C=O bond properties for the compounds analyzed here indicate that the greatest interaction energy is for centrosymmetric dimer **5**. It is also worth noticing that the shifts associated with the proton donor (N–H) are much larger than those of the acceptor group (C=O).

Results of DFT calculations

B3LYP/6-311++G(d,p) calculations were carried out on **1**, **3** and **5**, on isolated monomers as well as on centrosymmetric dimers connected through N–H···O hydrogen bonds (Fig. 6). Additionally, for comparison, calculations were performed for monomers and dimers not substituted by a moiety containing chlorine atoms (pyrrol-2-yl methyl ketone). Geometrical and energetic results concerning hydrogen bonds are given in Table 4. The hydrogen bond energies (E_{HB}) are exactly half of the binding energies since the dimers are linked through two symmetrically equivalent N–H···O interactions. One can observe that the lowest E_{HB} occurs for pyrrol-2-yl trichloromethyl ketone (**1**) dimer while for the remaining species the

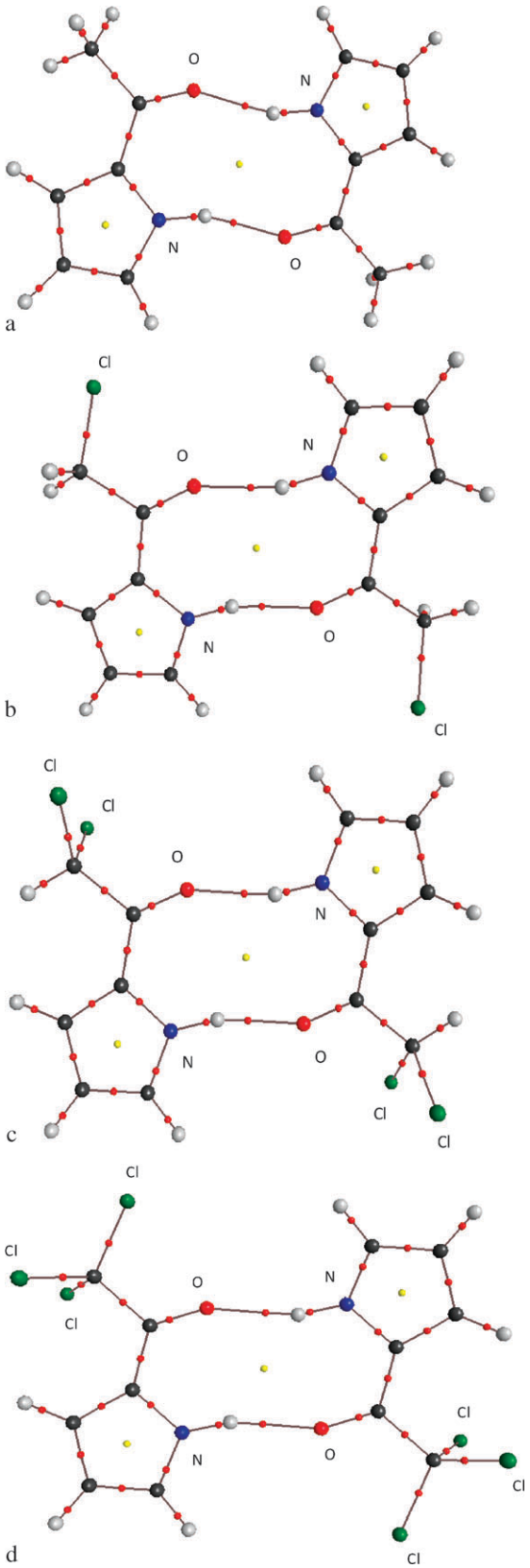

Fig. 6 Molecular structures of the dimers considered: (a) pyrrol-2-yl methyl ketone, (b) pyrrol-2-yl chloromethyl ketone, (c) pyrrol-2-yl dichloromethyl ketone, (d) pyrrol-2-yl trichloromethyl ketone. The bond paths are designated as well as attractors (big circles) attributed to nuclei; small circles designate critical points. O, N and Cl atoms are marked; unlabelled black and grey big circles correspond to C and H attractors, respectively.

differences in the hydrogen bond energies are practically negligible. This is reflected by H-bridge geometrical parameters (Table 4). It is well known that elongation of the proton donating bond and the proton acceptor distance are rough descriptors of hydrogen bonding strength.[28] For the species analyzed here (Table 4) the N–H bond length for monomers and dimers are 1.01 and 1.02 Å, respectively. This means that there is a slight bond elongation of ~0.01 Å as a result of complexation. This is rather typical for N–H proton-donating bonds where the elongation is not as meaningful as, for example, for O–H bonds.[43] The proton–acceptor distance is equal to 1.90 Å for the dimer of **1**, while for the remaining dimers the distance is 1.85–1.86 Å. This clearly confirms the previous statement that the weakest hydrogen bond occurs for compound **1**, while for the remaining species such energies are very close to each other. The N–H···O angles for all dimers considered (Table 4) are in the range 161–165°.

The energetic results are partly in line with vibrational spectra. As described in the previous section, the experimental values of $\Delta\nu_{N-H}$ are 116, 150 and 159 cm^{-1} (Table 1) for **1**, **3** and **5**, respectively, indicating the weakest hydrogen bond for the dimer of **1**. The order indicated by vibrational spectra, that fewer Cl atoms on the substituent correspond to stronger hydrogen bonding, is disturbed if H-bond energies are considered (see Table 4). However one can see that the $\Delta\nu_{N-H}$ shift is much less for **1** than for the remaining **3** and **5** dimers; these shift values are very close to each other for **3** and **5**. The theoretical shifts correspond to the experimental ones. There are also the very similar H-bond energies for the dimers considered, except for the dimer of **1** where the H-bond differs more and is the weakest one.

The natural bond orbitals (NBO) method[18] is also applied here. Table 4 presents the $n_Y \rightarrow \sigma_{XH}^*$ interaction energies connected with the maximum $n_Y \rightarrow \sigma_{XH}^*$ overlap. Such an interaction is responsible for the existence of X–H···Y hydrogen bond. n_Y designates the lone electron pair of the proton acceptor while σ_{XH}^* is an antibonding orbital of the proton-donating bond. The $n_Y \rightarrow \sigma_{XH}^*$ interaction is calculated as a second order perturbation theory energy according to the following relation (eqn (1)):

$$\Delta E(n_Y \rightarrow \sigma_{XH}^*) = -2\langle n_Y|F|\sigma_{XH}^*\rangle^2/(\varepsilon(\sigma_{XH}^*) - \varepsilon(n_Y)) \quad (1)$$

$\langle n_Y|F|\sigma_{XH}^*\rangle$ designates the Fock matrix element and $(\varepsilon(\sigma_{XH}^*) - \varepsilon(n_Y))$ is the orbital energy difference. The oxygen atom is the acceptor center for the dimers analyzed here, thus n_O oxygen lone pairs and σ_{XH}^* antibonding orbitals are taken into account.

The oxygen-accepting center is of sp^2 hybridization possessing two lone electron pairs. Hence there are two interaction energies corresponding to eqn (1) for each oxygen center. The two values are given in Table 4 in parentheses and also their sum is included (above the previously mentioned values). One can see that the lowest energies occur for **1** dimer while for the remaining dimers the values are similar to each other. The NBO results show again that the dimer of **1** has the weakest hydrogen bonds.

Table 5 shows the QTAIM results, characteristics of H···O bond critical point (BCP). It was found earlier that such characteristics may be treated as descriptors of hydrogen bond strength. Especially, the electron density at the proton-acceptor BCP (ρ_{BCP}) correlates well with the hydrogen bond energy.[13d,44] The differences between characteristics of BCPs for the considered dimers are not meaningful, for example ρ_{BCP} for dimer **1** is equal to 0.026 au while the value for the remaining dimers amounts to 0.028 au. One can observe that ρ_{BCP}, the Laplacian of electron density ($\nabla^2\rho_{BCP}$), the kinetic electron energy density at BCP (G_{BCP}) and the potential electron energy density at BCP (V_{BCP}) values are close to each other for dimers of **3**, **5** and pyrrol-2-yl methyl ketone, while these parameters for the dimer of **1** differ more. This is the same situation as that observed for geometrical and energetic values (see Table 4). Deeper analysis of V_{BCP} and G_{BCP} values shows that for all dimers G_{BCP} is always greater than the modulus of V_{BCP}. This means that H_{BCP}, the total electron energy density at BCP ($H_{BCP} = G_{BCP} + V_{BCP}$), is greater than zero. It was pointed out earlier that if H_{BCP} for BCP, corresponding to the proton–proton acceptor interaction within the hydrogen bridge, is negative the interaction may be classified as strong hydrogen bonding which is partially covalent in nature.[13] Such a situation is observed for centrosymmetric dimers of carboxylic acids.[11] However the N–H···O interactions, as H_{BCP} values show, are at most medium in strength. Fig. 6 shows the molecular structures of the dimers considered here; bond paths, attractors, bond critical points (BCPs) and ring critical points (RCPs) are presented. Fig. 7 presents the relief map of the electron density of pyrrol-2-yl methyl ketone. One can see the maxima corresponding to pyrrole rings; the maxima of the N–H···O connection are also shown. However not all maxima of H-atoms of the methyl groups are visible since the map was done in the plane of pyrrole rings.

It is worth mentioning that the electron density at RCP for all dimers presented in Table 4 and Table 5 amounts 0.0038 au. Since the parameters of RCP may also be considered as descriptors of hydrogen bond strength,[45] the latter observation shows that ρ_{RCP} is not sensitive to chlorine substituents. This is also partly in force for the remaining topological, geometrical and energetic parameters, except of the dimer of **1**; for the latter the parameters differ more from those of other dimers. The insight into the geometrical data

Table 4 Geometrical parameters of N–H···O hydrogen bonds (in Å and degrees), as well as H-bond energies (E_{HB}) and NBO energies, ΔE (both in kcal mol^{-1}); the corresponding N–H bond lengths for monomers are given in parentheses

Dimer	N–H	H···O	N···O	N–H···O	E_{HB}	ΔE
Pyrrol-2-yl methyl ketone	1.022 (1.010)	1.855	2.842	161.1	−6.23	13.33 (7.54; 5.79)
Pyrrol-2-yl chloromethyl ketone (**5**)	1.022 (1.010)	1.855	2.848	163.2	−6.45	12.81 (8.23; 4.58)
Pyrrol-2-yl dichloromethyl ketone (**3**)	1.022 (1.010)	1.847	2.843	164.2	−6.63	13.06 (8.71; 4.35)
Pyrrol-2-yl trichloromethyl ketone (**1**)	1.019 (1.010)	1.897	2.892	164.6	−5.26	11.21 (8.22; 2.99)

Table 5 Topological characteristics of (N)H···O BCP (in au)

Dimer	ρ_{BCP}	$\nabla^2\rho_{BCP}$	G_{BCP}	V_{BCP}
Pyrrol-2-yl methyl ketone	0.0283	0.1110	0.0253	−0.0229
Pyrrol-2-yl chloromethyl ketone (**5**)	0.0278	0.1112	0.0252	−0.0226
Pyrrol-2-yl dichloromethyl ketone (**3**)	0.0282	0.1131	0.0257	−0.0231
Pyrrol-2-yl trichloromethyl ketone (**1**)	0.0261	0.1088	0.0241	−0.0210

allows explanation of the latter characteristics. The bond lengths of $R_2^2(10)$ structural motif are presented in Table 6 (the N–H bond length of this motif is presented in Table 4). This structural motif contains two equivalent N–H···O hydrogen bonds and contains pairs of interacting atoms (C5═O, H···O, N–H, C1–N, C1–C5) and these pairs occur two times within the motif; thus there are 10 pairs of atoms (10 atoms within the ring closed by bonds and H···O interactions). Such rings occur for all dimers considered here (Fig. 6). Table 6 also shows C5–C6 bond lengths; these bonds are close to C–Cl bonds if chlorine substituents occur.

One can observe, for monomers, that there is no change of the above-mentioned bond lengths if the number of Cl substituents changes. The differences are within 0.01 Å. The only systematic changes are observed for C5–C6 bond directly connected with H or Cl atoms. The C5–C6 bond length is equal to 1.52, 1.53, 1.54 and 1.57 Å for pyrrol-2-yl methyl ketone, **5**, **3** and **1**, respectively. The similar systematic changes of C5–C6 are observed within dimers. For the remaining bonds of dimers there are no changes of bonds if the number of Cl substituents changes. If the bond lengths in monomers are compared with the corresponding ones in dimers, great changes are only observed for C═O and N–H (Table 4 and Table 6), which are directly involved in the hydrogen bond interaction. In the other words, the geometrical results show that Cl substituents do not change the $R_2^2(10)$ structural motif while the H-bond formation significantly changes only C═O and N–H bonds.

A quite different situation was observed for carboxylic acid dimers,[11] where complexation leads to π-electron delocalization and further to meaningful changes of bond lengths. It seems that the rigid skeleton of the pyrrole ring hampers π-electron delocalization; the C1–N bond length is practically the same and amounts to 1.38 Å for all monomers and dimers.

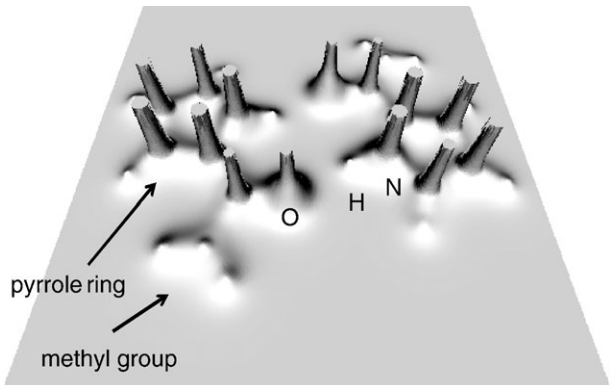

Fig. 7 Relief map of the electron density of the pyrrol-2-yl methyl ketone dimer expressed in the plane of pyrrole rings.

Table 6 Bond lengths (in Å) within the $R_2^2(10)$ structural motif containing two equivalent N–H···O bonds; the corresponding bond lengths for monomers are given in the lower line

Dimer	C5═O	C1–C5	C1–N	C5–C6
Pyrrol-2-yl methyl ketone	1.235	1.446	1.380	1.515
	1.225	1.461	1.378	1.515
Pyrrol-2-yl chloromethyl ketone (**5**)	1.228	1.443	1.381	1.528
	1.217	1.460	1.378	1.529
Pyrrol-2-yl dichloromethyl ketone (**3**)	1.227	1.435	1.382	1.538
	1.216	1.450	1.379	1.541
Pyrrol-2-yl trichloromethyl ketone (**1**)	1.222	1.437	1.385	1.576
	1.214	1.450	1.383	1.573

Table 7 presents NBO atomic charges for atoms of the $R_2^2(10)$ motif. The charges for monomers and dimers are shown. One can observe the following regularities. The oxygen acceptor atom becomes "more negative" and the H atom of the N–H proton-donating bond is "more positive" for dimers than for corresponding monomers. This is expected if hydrogen bonding is formed and it may be explained in the following way.[46] Hydrogen bonded species tend to adopt the linear X–H···Y arrangement since it corresponds to the strongest interaction and the maximum overlap for $n_Y \rightarrow \sigma_{XH}^*$. The increased occupancy of the σ_{XH}^* antibonding orbital causes the lengthening and weakening of X–H covalent bond (red shift of ν_{XH} stretching frequency). The maximizing of $n_Y \rightarrow \sigma_{XH}^*$ overlap is connected with the σ_{XH} bond repolarization and withdrawing the electron density from H-atom. Hence there is a diminishing of the electron density near the proton involved in hydrogen bonding. Generally, for most typical X–H···Y hydrogen bonds, one can observe the following consequences of hydrogen bond formation: there is a charge increase on the H atom (it is "more positive") and a charge decrease on the Y and X atoms (they are "more negative"). These tendencies have been observed in numerous studies (see for example the recent study of Pacios[47]). This is also observed in the case of the species considered here (Table 7), where as an effect of complexation there is a charge decrease of N-donor and O-acceptor centers as well as an increase of H-atom charge.

Generally there is electron charge transfer from a Lewis base to a Lewis acid;[48] in the case of hydrogen bonding interaction that is from the proton-accepting moiety to the proton-donating one.[49] Hence the proton-donating unit is negative while the proton-accepting one is positive within the H-bonded system. However repolarization effects result in the atomic charge distribution described above. For the complexes analyzed here both moieties act as proton donor and proton acceptor, and are symmetrically equivalent. This implies electron density symmetry. Hence both moieties are

Table 7 NBO charges (in au) of atoms within the $R_2^2(10)$ motif, the charges in dimers and in monomers are given, designations of atoms correspond to those of Scheme 1

Dimer	O	C5	C1	N	H	C6
Pyrrol-2-yl methyl ketone	−0.6568	0.5403	0.0059	−0.5075	0.4598	−0.6500
Pyrrol-2-yl chloromethyl ketone	−0.6314	0.5176	0.0043	−0.5048	0.4600	−0.4194
Pyrrol-2-yl dichloromethyl ketone	−0.6281	0.4960	0.0095	−0.5028	0.4610	−0.2688
Pyrrol-2-yl trichloromethyl ketone	−0.6163	0.4913	0.0010	−0.5031	0.4578	−0.2311
Monomer	O	C5	C1	N	H	C6
Pyrrol-2-yl methyl ketone	−0.5912	0.5223	0.0176	−0.5007	0.4243	−0.6581
Pyrrol-2-yl chloromethyl ketone (**5**)	−0.5599	0.5014	0.0143	−0.4980	0.4258	−0.4328
Pyrrol-2-yl dichloromethyl ketone (**3**)	−0.5533	0.4791	0.0177	−0.4960	0.4269	−0.2774
Pyrrol-2-yl trichloromethyl ketone (**1**)	−0.5461	0.4761	0.0068	−0.4956	0.4263	−0.2221

still neutral after complexation but typical X–H···Y charge distribution is observed.

For the carbon atom of the carbonyl group there is an increase of positive charge as a result of complexation. For the next carbon atom (C1) in the $R_2^2(10)$ motif there is a decrease of positive charge after the hydrogen bond formation, nitrogen becomes "more negative". The carbon atom (C6) that is located outside the above mentioned motif loses its electron charge, and to a greater extent if chlorine substituents are present. It is worth mentioning that within the N–H···O bridge, the O-atom is "less negative" and the H-atom is "less positive" if the number of Cl substituents increases. This may suggest a decrease in hydrogen bonding strength. It was shown here that this is detected by spectroscopic results and partly by energetic ones, since H-bond energy is lowest (its modulus) for pyrrol-2-yl trichloromethyl ketone dimer (**1**).

Conclusions

The results of spectroscopic investigations on conformations and intermolecular interactions of pyrrol-2-yl chloromethyl ketones (**1**, **3**, **5**) and their *N*-methyl derivatives (**2**, **4**, **6**) show the existence of two stable conformational forms in solution. NMR data correlate well with IR results and indicate that **1**, **3** and **5** are engaged in intermolecular hydrogen bonds. Compound **1** exhibits the weakest hydrogen bonding. These findings are supported by DFT results as well as QTAIM and NBO method. The DFT results show that the dimer of pyrrol-2-yl trichloromethyl ketone has the weakest hydrogen bonds, while the dimers of the remaining species have stronger hydrogen bonds which are all comparable in strength.

It is interesting that the $R_2^2(10)$ motif containing two equivalent N–H···O hydrogen bonds is hardly sensitive to the number of chlorine atoms. It seems that the rigid skeletons of the pyrrole rings hamper the π-electron delocalization within the above mentioned motif and thus the influence of the Cl substituents on the N–H···O hydrogen bond strength is strongly restricted for the pyrrole-2-yl chloromethyl ketones analyzed here. This is the reason why the N–H···O hydrogen bonds for these moieties are at most medium in strength. For example, for pyrrole-2-carboxylic acid, investigated previously,[6d,e,11] has medium strength N–H···O hydrogen bonds since they belong to the $R_2^2(10)$ motif found for the dimers analyzed here. However, there are also O–H···O hydrogen bonds between the linked carboxylic groups in the $R_2^2(8)$ motif. Since in the latter case there is π-electron delocalization, O–H···O hydrogen bonds are strong ones.

Acknowledgements

We would like to thank the Wroclaw Supercomputing and Networking Center (WCSS) for a generous allotment of computer time.

References

1 D. L. Snavely, F. R. Blackburn, Y. Ranasinghe, V. A. Walters and M. Gonzalez del Riego, *J. Phys. Chem.*, 1992, **96**, 3599.
2 (*a*) V. Lukeš, M. Breza and S. Biskupič, *Theor. Chem. Acc.*, 1999, **101**, 319; (*b*) R. C. Dunbar, *J. Phys. Chem. A*, 1998, **102**, 8946; (*c*) A. Pullman, G. Berthier and R. Savinelli, *J. Comput. Chem.*, 1997, **18**, 2012; (*d*) A. Pullman, G. Berthier and R. Savinelli, *J. Am. Chem. Soc.*, 1998, **120**, 8553.
3 (*a*) G. R. Desiraju and T. Steiner, *The Weak Hydrogen Bond in Structural Chemistry and Biology*, Oxford University Press, Inc., New York, 1999; (*b*) G. R. Desiraju, *Crystal Engineering: The Design of Organic Solids*, Elsevier, Amsterdam, 1989.
4 (*a*) S. L. Price, A. J. Stone, J. Lucas, R. S. Rowland and A. E. Thomleyt, *J. Am. Chem. Soc.*, 1994, **116**, 4910; (*b*) G. M. Day and S. L. Price, *J. Am. Chem. Soc.*, 2003, **125**, 16434; (*c*) P. Metrangolo and G. Resnati, *Chem.–Eur. J.*, 2001, **7**, 2511; (*d*) M. Formigué and P. Batail, *Chem. Rev.*, 2004, **104**, 5379; (*e*) F. Zordan, L. Brammer and P. Sherwood, *J. Am. Chem. Soc.*, 2005, **127**, 5979.
5 E. Bilewicz, A. Rybarczyk-Pirek, A. T. Dubis and S. J. Grabowski, *J. Mol. Struct.*, 2007, **829**, 208.
6 (*a*) A. T. Dubis and S. J. Grabowski, *J. Mol. Struct.*, 2001, **562**, 107; (*b*) A. T. Dubis and S. J. Grabowski, *New J. Chem.*, 2002, **26**, 165; (*c*) A. T. Dubis and S. J. Grabowski, *J. Phys. Chem. A*, 2003, **107**, 8723; (*d*) A. Dubis, S. J. Grabowski, D. B. Romanowska, T. Misiaszek and J. Leszczynski, *J. Phys. Chem. A*, 2002, **106**, 10613; (*e*) S. J. Grabowski, A. T. Dubis, D. Martynowski, M. Glówka, M. Palusiak and J. Leszczynski, *J. Phys. Chem. A*, 2004, **108**, 5815.
7 (*a*) M. C. Etter, *Acc. Chem. Res.*, 1990, **23**, 120; (*b*) M. C. Etter, J. B. Bernstein and J. C. McDonald, *Acta Crystallogr., Sect. B: Struct. Sci.*, 1990, **46**, 256.
8 A. F. L. O. M. Santos and M. A. V. Riberio da Silva, *J. Phys. Chem. A*, 2009, **113**, 9741.
9 S. J. Grabowski, A. T. Dubis, M. Palusiak and J. Leszczynski, *J. Phys. Chem. B*, 2006, **110**, 5875.
10 (*a*) R. F. W. Bader, *Acc. Chem. Res.*, 1985, **18**, 9; (*b*) R. F. W. Bader, *Chem. Rev.*, 1991, **91**, 893; (*c*) R. F. W. Bader, *Atoms in Molecules A Quantum Theory*, Oxford University Press, New York, 1990; (*d*) P. Popelier, *Atoms in Molecules An Introduction*, Prentice Hall, Pearson Education Limited, 2000; (*e*) *Quantum Theory of Atoms in Molecules Recent Progress in Theory and Application*, ed. C. Matta and J. J. Boyd, Wiley-VCH, 2007.
11 (*a*) R. W. Gora, S. J. Grabowski and J. Leszczynski, *J. Phys. Chem. A*, 2005, **109**, 6397; (*b*) S. J. Grabowski, *Croat. Chem. Acta*, 2009, **82**, 185.

12 S. J. Grabowski, W. A. Sokalski, E. Dyguda and J. Leszczynski, *J. Phys. Chem. B*, 2006, **110**, 6444.
13 (*a*) D. Cremer and E. Kraka, *Croat. Chem. Acta*, 1984, **57**, 1259; (*b*) S. Jenkins and I. Morrison, *Chem. Phys. Lett.*, 2000, **317**, 97; (*c*) W. D. Arnold and E. Oldfield, *J. Am. Chem. Soc.*, 2000, **122**, 12835; (*d*) I. Rozas, I. Alkorta and J. Elguero, *J. Am. Chem. Soc.*, 2000, **122**, 11154.
14 A. K. Tipton and D. A. Lightner, *Monatsh. Chem.*, 2002, **133**, 707.
15 M. S. Weiss, M. Brandi, J. Suhnel, D. Pal and R. Higenfeld, *Trends Biochem. Sci.*, 2001, **26**, 521.
16 A. T. Dubis and S. J. Grabowski, *Spectrochim. Acta, Part A*, 2002, **58**, 213.
17 (*a*) R. G. Parr and W. Yang, *Density Functional Theory of Atoms and Molecules*, Oxford, New York, 1989; (*b*) R. M. Dreizler and E. K. V. Gross, *Density Functional Theory*, Springer, Berlin, 1990; (*c*) W. Kohn, A. D. Becke and R. G. Parr, *J. Phys. Chem.*, 1996, **100**, 12974; (*d*) K. Müller-Dethlefs and P. Hobza, *Chem. Rev.*, 2000, **100**, 143; (*e*) G. Chalasinski and M. M. Szczęśniak, *Chem. Rev.*, 2000, **100**, 4227.
18 (*a*) A. E. Reed, L. A. Curtiss and F. Weinhold, *Chem. Rev.*, 1988, **88**, 899; (*b*) F. Weinhold and C. Landis, *Valency and Bonding, A Natural Bond Orbital Donor–Acceptor Perspective*, Cambridge University Press, Cambridge, 2005.
19 I. Nicolau and V. J. Demopoulus, *J. Heterocycl. Chem.*, 1998, **35**, 1345.
20 M. J. Frisch, G. W. Trucks, H. B. Schlegel, G. E. Scuseria, M. A. Robb, J. R. Cheeseman, V. G. Zakrzewski, J. A. Montgomery, Jr., R. E. Stratmann, J. C. Burant, S. Dapprich, J. M. Millam, A. D. Daniels, K. N. Kudin, M. C. Strain, O. Farkas, J. Tomasi, V. Barone, M. Cossi, R. Cammi, B. Mennucci, C. Pomelli, C. Adamo, S. Clifford, J. Ochterski, G. A. Petersson, P. Y. Ayala, Q. Cui, K. Morokuma, D. K. Malick, A. D. Rabuck, K. Raghavachari, J. B. Foresman, J. Cioslowski, J. V. Ortiz, A. G. Baboul, B. B. Stefanov, G. Liu, A. Liashenko, P. Piskorz, I. Komaromi, R. Gomperts, R. L. Martin, D. J. Fox, T. Keith, M. A. Al-Laham, C. Y. Peng, A. Nanayakkara, C. Gonzalez, M. Challacombe, P. M. W. Gill, B. G. Johnson, W. Chen, M. W. Wong, J. L. Andres, M. Head-Gordon, E. S. Replogle and J. A. Pople, *GAUSSIAN 98 (Revision A.6)*, Gaussian, Inc., Pittsburgh, PA, 1998.
21 M. J. Frisch, G. W. Trucks, H. B. Schlegel, G. E. Scuseria, M. A. Robb, J. R. Cheeseman, J. A. Montgomery, Jr., T. Vreven, K. N. Kudin, J. C. Burant, J. M. Millam, S. S. Iyengar, J. Tomasi, V. Barone, B. Mennucci, M. Cossi, G. Scalmani, N. Rega, G. A. Petersson, H. Nakatsuji, M. Hada, M. Ehara, K. Toyota, R. Fukuda, J. Hasegawa, M. Ishida, T. Nakajima, Y. Honda, O. Kitao, H. Nakai, M. Klene, X. Li, J. E. Knox, H. P. Hratchian, J. B. Cross, V. Bakken, C. Adamo, J. Jaramillo, R. Gomperts, R. E. Stratmann, O. Yazyev, A. J. Austin, R. Cammi, C. Pomelli, J. Ochterski, P. Y. Ayala, K. Morokuma, G. A. Voth, P. Salvador, J. J. Dannenberg, V. G. Zakrzewski, S. Dapprich, A. D. Daniels, M. C. Strain, O. Farkas, D. K. Malick, A. D. Rabuck, K. Raghavachari, J. B. Foresman, J. V. Ortiz, Q. Cui, A. G. Baboul, S. Clifford, J. Cioslowski, B. B. Stefanov, G. Liu, A. Liashenko, P. Piskorz, I. Komaromi, R. L. Martin, D. J. Fox, T. Keith, M. A. Al-Laham, C. Y. Peng, A. Nanayakkara, M. Challacombe, P. M. W. Gill, B. G. Johnson, W. Chen, M. W. Wong, C. Gonzalez and J. A. Pople, *GAUSSIAN 03 (Revision B.03)*, Gaussian, Inc., Wallingford, CT, 2004.
22 A. D. Becke, *J. Chem. Phys.*, 1993, **98**, 5648.
23 (*a*) A. D. McLean and G. S. Chandler, *J. Chem. Phys.*, 1980, **72**, 5639; (*b*) M. J. Frisch, J. A. Pople and J. S. Binkley, *J. Chem. Phys.*, 1984, **80**, 3265; (*c*) R. Krishnan, J. S. Binkley, R. Seeger and J. A. Pople, *J. Chem. Phys.*, 1980, **72**, 650; (*d*) T. Clark, J. Chandrasekhar, G. W. Spitznagel and P. V. R. Schleyer, *J. Comput. Chem.*, 1983, **4**, 294.
24 A. Frish, A. B. Nielsen and A. J. Holder, *Gaussview User Mannual*, Gassian Inc., Pittsburg, PA, 2000.
25 S. F. Boys and F. Bernardi, *Mol. Phys.*, 1970, **19**, 553.
26 *AIM2000 designed by Friedrich Biegler- König*, University of Applied Sciences, Bielefeld, Germany, 2000.
27 I. V. Alabugin, M. Manoharan, S. Peabody and F. Weinhold, *J. Am. Chem. Soc.*, 2003, **125**, 5973.
28 (*a*) G. A. Jeffrey, *An Introduction to Hydrogen Bonding*, Oxford University Press, New York, 1997; (*b*) S. J. Grabowski, *Tetrahedron*, 1998, **54**, 10153.
29 J. Kauppinen, D. Moffat, H. Mantsch and D. Cameron, *Anal. Chem.*, 1981, **53**, 1454.
30 I. Karaamancheva and T. Staneva, *J. Pharm. Biomed. Anal.*, 2000, **21**, 1161.
31 P. A. Gale, S. Camiolo, G. J. Tizzard, C. P. Chapman, M. E. Light, S. J. Coles and M. B. Hursthouse, *J. Org. Chem.*, 2001, **66**, 7849.
32 D. J. Chadwick and I. A. Cliffe, *J. Chem. Soc., Perkin Trans. 2*, 1980, 737.
33 P. Bruni, E. Giorgini, E. Maurelli and G. Tosi, *Vib. Spectrosc.*, 1996, **12**, 249.
34 Q. Liu, X. Xu and W. Sang, *Spectrochim. Acta, Part A*, 2003, **59**, 471.
35 Ch. L. Cheng, I. G. John, G. L. D. Ritchie and P. H. Gore, *J. Chem. Soc., Perkin Trans. 2*, 1974, 1318.
36 C. Conti, R. Galeazzi, E. Giorgini and G. Tossi, *J. Mol. Struct.*, 2005, **744–747**, 417.
37 S. Xu, Ch. Wang, G. Sha, J. Xie and Z. Yang, *THEOCHEM*, 1999, **459**, 163.
38 R. M. Badger and S. H. Bauer, *J. Chem. Phys.*, 1937, **5**, 839.
39 C. N. R. Rao, P. C. Dwivedi, H. Ratajczak and W. J. Orville-Thomas, *J. Chem. Soc., Faraday Trans. 2*, 1975, **71**, 955.
40 R. S. Macomber, *A Complete Introduction to Modern NMR Spectroscopy*, J. Wiley & Sons, Inc., Toronto, 1998.
41 A. D. Buckingham, J. E. Del Bene and S. A. C. McDowell, *Chem. Phys. Lett.*, 2008, **463**, 1.
42 J. E. Del Bene, W. B. Person and K. Szczepaniak, *Mol. Phys.*, 1996, **89**, 47.
43 P. Gilli, V. Bertolasi, V. Ferretti and G. Gilli, *J. Am. Chem. Soc.*, 1994, **116**, 909.
44 (*a*) O. Mó, M. Yánez and J. Elguero, *J. Chem. Phys.*, 1992, **97**, 6628; (*b*) O. Mó, M. Yánez and J. Elguero, *THEOCHEM*, 1994, **314**, 73; (*c*) E. Espinosa, E. Molins and C. Lecomte, *Chem. Phys. Lett.*, 1998, **285**, 170; (*d*) O. Galvez, P. C. Gomez and L. F. Pacios, *Chem. Phys. Lett.*, 2001, **337**, 263; (*e*) O. Galvez, P. C. Gomez and L. F. Pacios, *J. Chem. Phys.*, 2001, **115**, 11166; (*f*) O. Galvez, P. C. Gomez and L. F. Pacios, *J. Chem. Phys.*, 2003, **118**, 4878; (*g*) L. F. Pacios, *J. Phys. Chem. A*, 2004, **108**, 1177.
45 S. J. Grabowski and M. Małecka, *J. Phys. Chem. A*, 2006, **110**, 11847.
46 F. Weinhold and C. Landis, *Valency and Bonding, A Natural Bond Orbital Donor–Acceptor Perspective*, Cambridge University Press, Cambridge, 2005, pp. 595.
47 L. F. Pacios, Changes of Electron Properties in the Formation of Hydrogen Bonds, in *Hydrogen Bonding New Insights*, ed. S. J. Grabowski, Springer, Dordrecht, 2006, ch. 3.
48 P. Lipkowski, S. J. Grabowski and J. Leszczynski, *J. Phys. Chem. A*, 2006, **110**, 10296.
49 S. Scheiner, *Hydrogen Bonding. A Theoretical Perspective*, Oxford University Press, Oxford, 1997.

